JOURNAL OF THE KOREAN ASTRONOMICAL SOCIETY
**38**: 17 ∼ 22, 2005

# A NEW REFERENCING METHOD FOR THE ARRAY ON-THE-FLY OBSERVATION

EUN JUNG CHUNG[1,2], HYORYOUNG KIM[2], AND MYUNG-HYUN RHEE[3]
[1]Dept. of Astronomy, Yonsei University, Seoul 120-749, Korea
[2] Taeduk Radio Astronomy Observatory, KASI, Daejeon 305-348, Korea
[3] Yonsei University Observatory, Yonsei University, Seoul 120-749, Korea
*E-mail: rigel@galaxy.yonsei.ac.kr, hrkim@trao.re.kr, and rhee@obs.yonsei.ac.kr*
*(Received February 20, 2005; Accepted March 12, 2005)*

## ABSTRACT

In this paper, we suggest a new referencing method for the array On-The-Fly(OTF) observations in radio astronomy. To reduce the baseline residual, we have proposed and evaluated a new referencing method which uses the source free regions in the observed frame as references. These new references have small $\triangle t$ and $\triangle x$, the time and position differences between the source and the references, and the systematic problems were improved by using this new referencing method. The curved baseline residuals were straightened and the rms was reduced to 17 mK. This new referencing method is expected not only to make possible to take more stable data for the array OTF observation of external galaxies but also to save the observation and data reduction time.

*Key words :* OTF Observation – galaxies : individual(NGC 4254) – techniques : image processing

## I. INTRODUCTION

On-The-Fly observation mode in radio astronomy is one of results of the astronomers' efforts to improve the observational techniques. Most single dish observations are performed with step-and-integrate mode in which the antenna observes a galaxy at several points along the major-axis (and other points if it is needed). But because of the long exposure time, there are some difficulties to remove the atmospheric and systemic effects. OTF observation mode drives the telescope smoothly and rapidly across a field storing data and antenna position information continuously. Due to its fast moving and covering the whole observational region in short observing time, OTF observation has several advantages to the classical step-and-integrate observation. The first is the reduction of telescope overhead. The second is that the properties of the atmosphere and the system change less in comparison to a conventional step-and-integrate mapping method (Mangum 1999). And economy of observing time is also one of the OTF observation's advantages.

Referencing is very important to subtract baseline in radio observation, and there are two commonly used referencing methods for the OTF observation. The first is position-switching method. Position-switching method is similar with that of classical step-and-integrate observation in which references are generally obtained in azimuth every several seconds at the region between 5′ and 10′ from the object's center (e.g., Young et al. 1995). In OTF observation, references are also taken at a distance from the center followed by one or more total power scanning rows and one or more consecutive source positions were shared with a single off-source reference. But, when atmospheric condition changes rapidly, off-source references and the source frame do not have the same sky value. Standard chopper wheel method (Penzias & Burrus 1973) have been also used in OTF observation, in which the subreflector is switched between the two reference positions in azimuth while the telescope scans.

Those referencing method mentioned above performed their part most effectively until now, but they are not enough to serving the purposes of OTF observation and could get some systematic problems. OTF observation mode minimizes the cumulated atmospheric and systemic uncertainties of the classical step-and-integrate observation due to the long exposure time at a position by shortening the exposure time and increasing the redundances. But the two referencing methods still have too long exposure time at the reference positions in comparison with the scanning time of a source point in OTF mode. Scanning time of the observing source region is about 0.1 ∼ 1 seconds per a point, but that of the reference region is about 5 ∼ 20 seconds (FCRAO OTF Manual; http://donald.astro.umass.edu/∼fcrao, Mangum 1999). They cannot give the satisfiable information about the fast changing sky and systems, but also they might hinder sky subtraction and make some false structures. In this paper, we propose a new referencing method. Section 2 presents that what the problem of our observation data is and how we made a trial to solve it. Section 3 describes that the analysis of the cause. On the basis of the analysis, we propose a new referencing method in Sec.4. We compare the datacube which was taken using the new referencing method with that using the conventional referencing

*Corresponding Author*: M.-H. Rhee

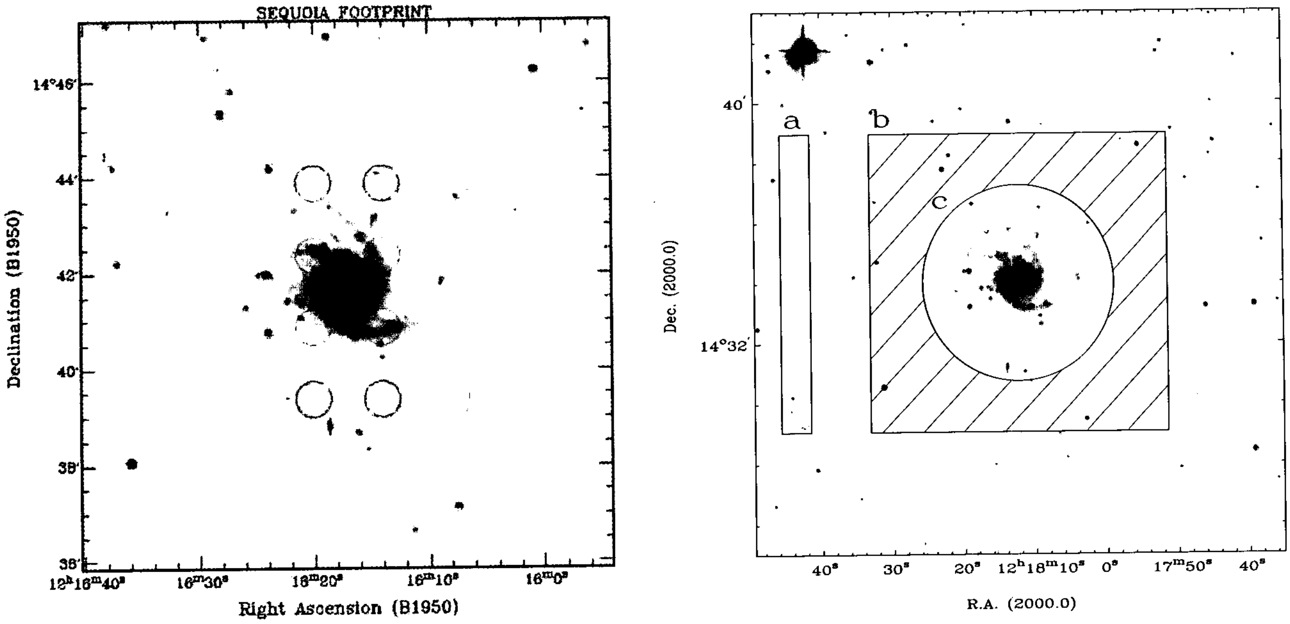


**Fig. 1.**— LEFT : Configuration of SEQUOIA and its sky-coverage. The separation between adjacent horns is 88″ and the diameter of a horn is 44″. In dual polarization, the top and bottom rows are from second polarization. RIGHT : ONs and OFFs. Rectangle (a) is OFFs as references and rectangle (b) is ONs which is the summation of the sources and references. The shaded region (c) is inner source free region which will be used as references in our new referencing method in section 4.

method, and detail the results. Discussion and conclusion are in section 5.

## II. A SYSTEMIC PROBLEM OF OUR OBSERVATION

### (a) Observation

We carried out the array OTF observations of 28 Virgo cluster galaxies using 14m telescope of the Five College Radio Astronomy Observatory (FCRAO) from 7 observational runs during 17-27 Jan., 16-24 Feb., 15-19 Mar., 27 Nov. - 1 Dec., 19-20 Dec. 2002, and 24-27 Feb. 2003 as our Virgo Cluster Survey Project(Chung 2003; Kim 2003). To increase the detection rate of CO, we selected strong global CO flux, $S_{CO}$, and dynamically quiescent galaxies among the Virgo Cluster galaxies. The sample is not really large, but it has advantages which provides a well-defined, volume limited, and equidistant sample.

FCRAO telescope is Cassegrain design antenna and has a SEQUOIA which is the focal plane array receiver (Fig.1). It contains 16 horns with 44″ beam size and configure 4 × 4 array. The backend of the receiver utilizes QEF (Quabbin Extra galaxy Filterbank), consisting of sixteen 64 channel and 5 MHz resolution filter banks, providing 320 MHz of available bandwidth. Spectra were calibrated by the standard chopper-wheel method which corrects for atmospheric (to first order) and ambient temperature losses to yield the corrected antenna temperature $T_A^*$.

Every galaxies had mapped of 10′ × 10′ size(ONs, rectangle (b) in the right figure of Fig.1). The antenna moved at 45″ per second, and the data were stored in every 0.25 seconds. References were obtained at the position with 30 arcminute offset in the azimuth direction(OFFs, rectangle (a) in the right figure of Fig.1). The pointing and focus of the telescope were measured normally at the beginning of each observing run, and occasionally during the middle of the run when the weather condition varies much. We have measured an rms pointing error of ∼ 3″ in both azimuth and elevation, or ∼ 5″ total. The pointing source is R-LEO with rest frequency 86.243442 GHz.

### (b) Data Acquisition and a Systemic Problem

We synthesized the raw datacubes in OTF tool. Each OTF raw data consists of hundreds of qef files, and each qef file contains 135 samples. For each galaxy, we picked out bad data of the samples, and calibrated and regridded only with the remained good samples on the basis of the floating level, rms, trajectory, elevation, and $T_{sys}$. And we applied the conventional references(OFFs) to each datacube. We used jinc-gaussian function to regrid, and fixed the cell size to be 15″ and baseline order 2 (Kim 2003).

We found that the every raw datacubes taken from this processes in OTF tool had hockey stick shaped baseline which were seemed to be caused by systemic ef-

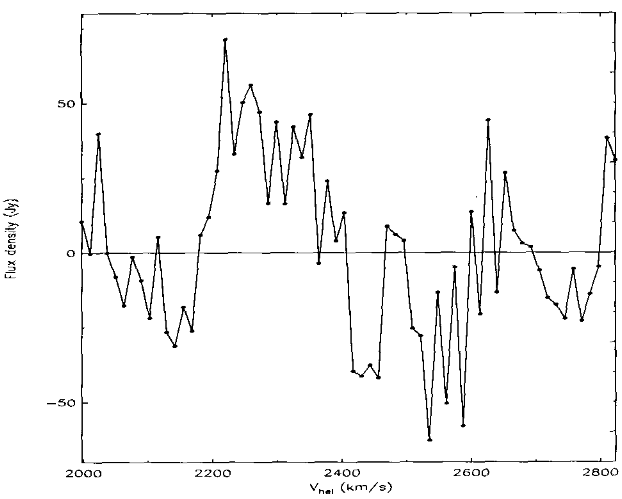


**Fig. 2.**— Global profile of NGC4254 : the channel baseline is excessively bent. From the fact that most galaxies have this curved baseline shape, the cause seems to be the systematic effects.

fects(see Fig.2). To remove this systemic effect, we used median-filtering task in AIPS (Astronomical Image Processing System; http://www.cv.nrao.edu/aips/) and continuum remove task and blot task in GIPSY (Groningen Image Processing SYstem; http://www.astro.rug.nl/gipsy/; van der Hulst et al. 1992). After reducing the data using these tasks, the channel baselines of galaxies were gotten better than before. But these data reduction processes can cause the transformation and distortion of data, and the original problems are not solved and still remained.

## III. ANALYSIS OF THE CAUSE

To analyze the causes of the systemic effects, we look into the spectrum data reduction algorithm of the differential measurement. First of all, when observing a celestial objects, the antenna receives the electromagnetic waves not only from the source but also from the sky. If we call the spectrum of the source $S_{src}$, and the other effects $S_{ref}$, then we can write the spectra which come from the ON and OFF become

$$S_{ON} = S_{src} + S_{ref}, \tag{1}$$

$$S_{OFF} = S_{ref}, \tag{2}$$

$$\triangle S = S_{ON} - S_{OFF}. \tag{3}$$

The second, the acquired data was affected by the instruments we used. Therefore,

$$S_{obs}(\nu, t, \vec{x}) = I(\nu, t) \odot F(\nu, t, \vec{x}), \tag{4}$$

where $S_{obs}(\nu, t, \vec{x})$ is the observed spectrum, $F(\nu, t, \vec{x})$ is the flux arriving at the ground, and $I(\nu, t)$ is the instrumental reaction function. The variable t is time, $\nu$ is frequency, and $\vec{x}$ is the position on the celestial sphere (see i.e. Tools of radio astronomy and An Introduction to the radio astronomy).

To simplify the equation, we assume that the variations by the frequencies can be ignored, then the equation (4) becomes

$$S_{obs}(t, \vec{x}) = I(t) \odot F(t, \vec{x}). \tag{5}$$

$$\begin{aligned} \triangle S &= S_{ON} - S_{OFF} \\ &= I(t_1) \odot [F_{src}(t_1, \vec{x_1}) + F_{ref}(t_1, \vec{x_1})] \\ &\quad -I(t_2) \odot F_{ref}(t_2, \vec{x_2}) \end{aligned} \tag{6}$$

where $t_1$ and $\vec{x_1}$ are the time and position of ONs, and $t_2$ and $\vec{x_2}$ are those of OFFs.

For the instrumental reaction function and the flux, we can write the approximated equation as follows

$$I \equiv I(t_1), \tag{7}$$

$$F \equiv F(t_1, \vec{x_1}), \tag{8}$$

$$I(t_2) \approx I + \frac{\partial I}{\partial t}\triangle t, \tag{9}$$

$$F(t_2, \vec{x_2}) \approx F + \frac{\partial F}{\partial t}\triangle t + \frac{\partial F}{\partial x}\triangle x. \tag{10}$$

Substituting these to equation (6),

$$\begin{aligned} \triangle S &\approx I \odot [F_{src} + F_{ref}] \\ &\quad -[I + \frac{\partial I}{\partial t}\triangle t] \odot \\ &\quad [F_{ref} + \frac{\partial F}{\partial t}\triangle t + \frac{\partial F}{\partial x}\triangle x]. \end{aligned} \tag{11}$$

The $\triangle t \triangle x$ can be ignored, then

$$\begin{aligned} \triangle S &\approx I \odot F_{src} \\ &\quad -[I \odot \frac{\partial F}{\partial t} + \frac{\partial I}{\partial t} \odot F_{ref}]\triangle t \\ &\quad -I \odot \frac{\partial F}{\partial x}\triangle x. \end{aligned} \tag{12}$$

And the variations of $\triangle S$, $\delta(\triangle S)$, is

$$\delta(\triangle S) = [I \odot \frac{\partial F}{\partial t} + \frac{\partial I}{\partial t} \odot F_{ref}]\triangle t + [I \odot \frac{\partial F}{\partial x}]\triangle x. \tag{13}$$

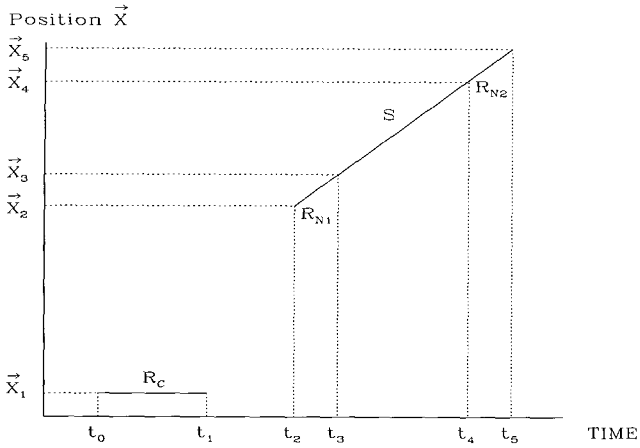


**Fig. 3.**— Time & position passages of source(S), conventional outer reference($R_C$), and new inner reference($R_{N1}$ and $R_{N2}$) in a row sampling : the time($t_0 \sim t_5$) required for one row sampling is about 22 seconds. The distance between the conventional reference($X_1$) and the source region($X_2$) is about 12′. The total observing region is 10′ × 10′.

As shown above, we can explain that the variations of the spectrum is caused by the large $\triangle t$ and $\triangle x$, and if we make $\triangle t$ and $\triangle x$ become smaller, the effect will be also decreased.

## IV. A NEW REFERENCING METHOD

### (a) Proposal of a New Referencing Method

To minimize the $\triangle t$ and $\triangle x$, we propose to use the inner source free region as references instead of the outer source free region. See right figure of Fig.1 again. The rectangle (b) is the target source frame, and rectangle (a) is the conventionally used reference frame. We suggest to use the shaded region (c), inner source free region, which has no emission but near from the source emission.

Fig.3 is the time and position diagram of observation which shows the time and positions of the source, conventional references, and the new references. In our classical OTF observation, the conventional reference($R_C$ ; $\vec{X_1}$) and the source region(S ; $\vec{X_2} \sim \vec{X_5}$) are observed alternately. The time taken a reference and source($t_0 \sim t_5$), one row sampling, is 22 seconds, and the integration time on reference position($t_0 \sim t_1$) is 5 seconds. The position difference between conventional references and the source is about 12′. These mean that the conventional references and the source have differences in time and position, and these differences can take the changes of systemic and atmospheric

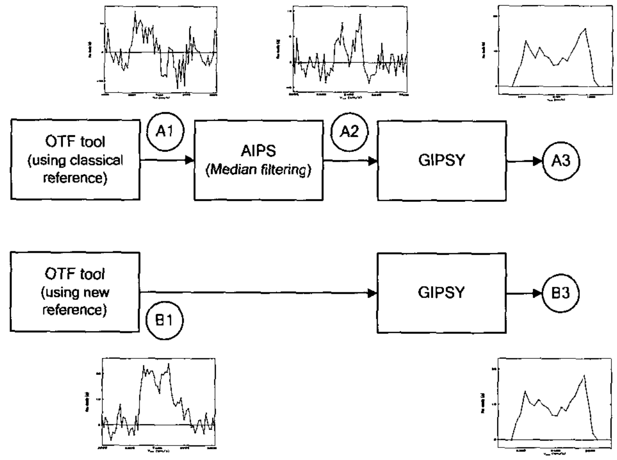


**Fig. 4.**— Data reduction flow chart : A1 and B1 are raw datacubes taken from OTF tool using conventional and new references respectively. A2 is median-filtered datacube in AIPS to stretch the curved baseline. A3 and B3 are the final datacubes followed by the same data reduction steps in GIPSY. And both of them show clear zero level baseline after the BLOT task in GIPSY. Note that B1 skips the median-filtering works in AIPS, and reduction of B1 in GIPSY is done directly by the same procedures with A2. The spectra in each reduction step show the transitions of channel baselines by reduction processes.

conditions. But, the new references($R_{N1}$ and $R_{N2}$ ; $\vec{X_2} \sim \vec{X_3}$ and $\vec{X_4} \sim \vec{X_5}$) are included in the source. Therefore the reference and the source have little difference of the time and position, and their systemic and atmospheric conditions are much alike each other. For these similar systemic and atmospheric conditions due to the closer time and position, the new referencing method might be more suitable for the OTF observation, and it is expected to be a solution of the systemic effects.

### (b) Comparisons between the Conventional and the New Referencing Methods

To compare the effects of the references, we chose NGC 4254 and reduced the data with two phases using two different references. NGC 4254, Sc galaxy, locates at the northwest 3.6° far away from M87, and it was reported as it has a very asymmetric HI distribution (Cayatte et al. 1990). But it does not show so much asymmetry in spatial distribution in CO image (Kim 2003). NGC 4254 was mapped of 10′ × 10′ size like other galaxies and it was iterated 14 times. The source elevation changed between 33 ∼ 62 degrees during the observations. $T_{sys}$ varied between 300 ∼ $600K$ with typical value of 400 K. NGC 4254 is very suitable to check the effects of the new referencing method, be-

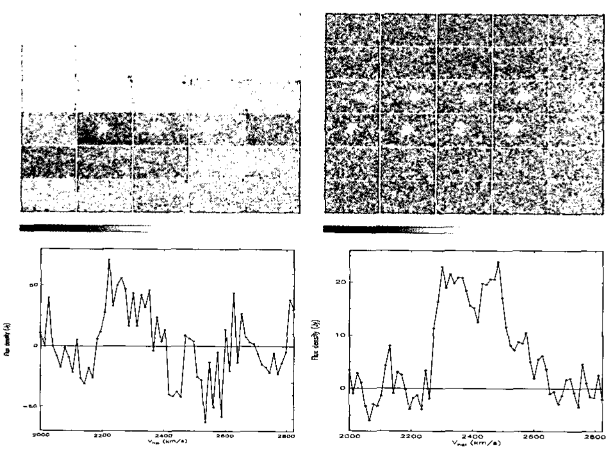

**Fig. 5.**— Channel maps(top) and global profiles(bottom) of A1(left) and B1(right) : the conventional and new references were applied to them respectively in OTF tool. Channel separation of channel maps is $\sim 26km/s$ and that of global profiles is $\sim 13km/s$. Both channel map and global profile of A1 show serious gradient between channels, but those of B1 show very flat channel baseline.

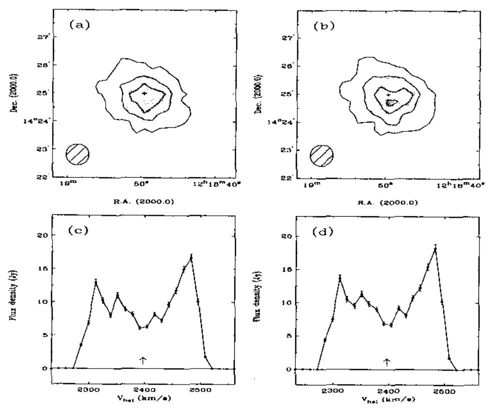


**Fig. 6.**— CO map and global profile to compare the two final datacubes : (a) CO map of A3, (b) CO map of B3, (c) CO global profile of A3, (d) CO global profile of B3. The two final results from different referencing methods and data reduction processes are similar.

cause it has small rms (about 18 mK) and its emission is very obvious.

The reduction processes are presented in Fig.4. A and B denote the references applied to each datacube; A the conventional references and B the new references. The numbers indicate the stages of the reduction; 1 of A and B the pre-reduction in OTF, 2 of A the reduction in AIPS, and 3 of A and B the reduction in GIPSY. From the comparison between A and B, we can verify the effects of references. And we can check that using the new referencing method never distort the data extraordinarily by the comparisons between final datacubes.

We synthesized the raw datacubes in OTF tool with the same procedures explained in Sec. 2. However we applied different references to the datacubes, the conventional references for A1 and the new inner source free references for B1 as Fig.4 shows. Before choosing the new reference region for B1, we checked first whether the region is perfectly clear or not. We used jinc-gaussian function to regrid, and fixed the cell size to be $15''$ and baseline order 2. We reduced the raw datacube A1 and B1 in AIPS and GIPSY. AIPS procedure is applied to A1 only, and GIPSY procedure is applied to both datacubes.

Fig.4 shows the differences and transitions of the data by reduction processes. When using different referencing methods in pre-reduction step of OTF tool, there exist differences between the global profiles of A1 and B1. Fig.5 shows these differences more obviously. A1 has serious baseline gradient which is almost hockey stick shaped in both channel map and global profile. But, it is perfectly straightened for the data B1 applied the new referencing method. From the comparison between A1 and A2, we can see that the median-filtering work in AIPS crooks the original data severely though the hockey stick shaped channel baseline was improved in A2 after the work in AIPS.

A3 and B3 of Fig.4 are final results of data pre-reduction and reduction processes. Their comparisons are reported in Fig.6 in detail. The (a) and (c) are CO contour map and global profile of A3, and the (b) and (d) are of B3. We can check that the CO contour maps and global profiles of A3 and B3 have very similar shapes with each other. Table 1. helps us to understand the comparisons of the results quantitatively. There is a great differences of $S_{CO}$ and rms level between the raw data A1 and B1. But the large discrepancies between them decrease at the final stage. The rms level is same as 15mK, and the difference of $S_{CO}$ between A3 and B3 is also decreased about a third of that between A1 and B1.

## V. SUMMARY & CONCLUSION

Our OTF observation data showed a systematic problem of the hockey stick shaped channel baseline, and we analyzed the causes of the problem by differential measurements. To decrease the $\Delta t$ and $\Delta x$ between the source and the references, we used inner source free region as references instead of the conventionally used outer source free region references. When using the new referencing method, the systematic problem presented at the data using the conventional references was improved. The curved baseline was flattened

TABLE 1.
$S_{CO}$ AND RMS OF EACH DATACUBES

| | A1 | B1 | A3 | B3 |
|---|---|---|---|---|
| $S_{CO}$ (Jy Km/s) | 2090±60 | 2440±50 | 2110±40 | 2280±40 |
| rms (K) | 0.021 | 0.017 | 0.015 | 0.015 |

and the rms was reduced. These are very encouraging results in two respects. The first is that the new referencing method minimizes the variations of data in the reduction processes and gives very stable datacubes. The second is that it can also give better data of which rms is small. We can expect that the observations of the weak CO galaxies are more effective by using this new referencing method.

The new referencing method has several advantages over the conventional referencing method. The first advantage is that the reduction process becomes more simple and clear by using the new referencing method. When using the conventional references, more time and efforts are needed to do the median-filtering in AIPS. It is a little annoying works to get the fits file into AIPS, median-filtering, rewriting into fits file, and putting it into GIPSY. If we use the new referencing method, these steps are omissible, and reduction time and efforts can be saved. The second is the safety of choosing the referencing regions for the compact source observations such as external galaxies. For the array OTF, the 16 horns move together as one, it is difficult to find clear reference region for the whole 16 horns. And even if the fixed reference region has small emission, then it will take very serious problems. But, if we use the new referencing method, it will become easier to find the clear references for the array horns. Besides this, we always ascertain that the references has no emission. The third advantage is to save the observation time. The time to get the references by position-switching mode is different according to the observing parameters. Even so, using the inner source free regions as references saves the observation time. In case of observation which takes 5 seconds for references during 22 seconds for a cycle of source and reference, using the inner source free regions saves the time about 25%.

This new referencing method which uses the inner source free regions as references can be easily applied to the established facilities like FCRAO. And we expect this new referencing method is still more useful to the observation of faint sources and/or complex systems such as interacting galaxies. Therefore if this is applied to the antenna systems of higher sensitivity like LMT, it can be more effective. Besides these, TRAO (Taeduk Radio Astronomy Observatory) and SRAO (Seoul Radio Astronomy Observatory) have a plan to apply this referencing method after OTF observation mode is realized, and the application of domestic antennas will be increased.

We will check the usability of this method by applying it to our other Virgo cluster galaxies, and investigate the effects of the new referencing method statistically.

## REFERENCES

Burke, B. F., & Graham-Smith, F. 1997, An Introduction to radio astronomy (Cambridge University Press)

Cayatte, V., van Gorkom, J. H., Balkowski, C., & Kotanyi, C. 1990, VLA observations of neutral hydrogen in Virgo Cluster galaxies. I - The Atlas, AJ, 100, 604

Chung, E. J. 2003, CO Tully-Fisher Relation in the Cluster Galaxies, M.S. Thesis, Yonsei University

Heyer, M. H., Narayanan, G., & Brewer, M. 2001, On The Fly Mapping at the FCRAO 14m Telescope (User's Manual)

Kenney, J. D. P., & Young, J. S. 1988, CO observations of all Virgo Cluster spiral galaxies brighter than B(T) exp 0 = 12, ApJS, 66, 261

Kim, H. 2003, CO Imaging Survey of Virgo Cluster Spirals, PhD Thesis, Pusan National University

Mangum, J. 1999, On the Fly Observing at the 12m (User's Manual)

Penzias, A. A., & Burrus, C. A. 1973, Millimeter-Wavelength Radio-Astronomy Techniques, ARA&A, 11, 51

Rohlfs, K., & Wilson, T. L. 2000, Tools of radio astronomy (3rd edn; Springer-Verlag)

van der Hulst et al. 1992, in Astronomical Data Analysis Software and Systems I, A.S.P. Conference Series, Vol. 25, 1992, Diana M. Worrall, Chris Biemesderfer, and Jeannette Barnes, eds., p. 131.

Young, J. S. et al. 1995, The FCRAO Extragalactic CO Survey. I. The Data, ApJS, 98, 219